

Electronic Supplementary Information

In situ formic acid dehydrogenation observation using UV-vis-diffuse-reflectance spectroscopy system

Risheng Li,^{ab} Tetsuya Kodaira,^{b*} Hajime Kawanami^{ab*}

^a Graduate School of Pure and Applied Science, University of Tsukuba, 305-8577, Japan

^b National Institute of Advanced Industrial Science and Technology (AIST), 305-8565, Japan

1. General Experimental Procedures

1.1 Reagents.

All reagents were purchased from following companies.

Reagent	Company
formic acid (98% mass/mass)	FUJIFILM Wako Pure Chemical Corporation
deionized water	Purified by Direct-Q UV 5, Merck Millipore
sulfuric acid (95.0 % mass/mass)	FUJIFILM Wako Pure Chemical Corporation
α -Al ₂ O ₃ [99.99%]	Kojyundo Chemical Laboratory Co. Ltd.
γ -Al ₂ O ₃ [99.89%]	Mizusawa Industrial Chemicals Ltd.
TiO ₂ (P25) †	Evonik Industries (Nippon Aerosil Co., Ltd.)
SiO ₂ (Si60)	Kanto Chemical Co., Inc.
Monoclinic ZrO ₂	Daiichi Kigenso Kagaku Kogyo Co., Ltd.
[Cp*Ir(H ₂ O) ₃][SO ₄]	STREM Chemicals Inc.
4,4'-Dihydroxy-2,2'-bipyridine	FUJIFILM Wako Pure Chemical Corporation
Alizarin	FUJIFILM Wako Pure Chemical Corporation

† Calcined at 1100 °C to convert fully into highly crystalline rutile.

1.2 The synthesis of [Cp*Ir(4DHBP)(OH₂)]SO₄

20 mL of methanol was added to an aqueous solution (20 mL) of [Cp*Ir(H₂O)₃][SO₄] (0.12 mmol) and 4,4'-dihydroxy-2,2'-bipyridine (0.12 mmol), and the solution was stirred for 12 hours with N₂ purging at room temperature. After the reaction, the solution was concentrated to 5 mL and then stored in a refrigerator at 5 °C for 12 hours followed by the filtration and then the yellow precipitate was collected. Finally, 1.45 g (yield 92.1%) of a yellow solid ([Cp*Ir(4DHBP)(OH₂)]SO₄) was obtained after 12 hours of drying in vacuo.

1.2 Analytical apparatus.

Transmission UV-Vis spectra were measured by Cary 60 UV-Vis spectrometer (Agilent Technology Inc.) equipped with a fiber probe. During the FADH reaction catalyzed by ([Cp*Ir(4DHBP)(OH₂)]SO₄) (reaction temperature: 80 °C). The fiber probe was inserted into the reactor to conduct the measurement. SEM images and particle size distribution were obtained using SU9000 (Hitachi Co. Ltd.) and SALD-7500 (Shimadzu), respectively. Average particle size was calculated from the resultant data of SALD-7500 as well as the images from SEM. The formic acid concentration of the solution after reaction was determined by liquid chromatography (Agilent Technologies, 1260 Infinity II equipped with Shodex RSpak KC-811, aqueous diluted HClO₄ as an eluent).

1.3 Measurement procedures of UV-Vis diffuse-defraction absorption of alizarin

Absorption spectra of alizarin,[1] were measured by the following procedures. Desired amount of alizarin (2.27 mg in 25 mL of deionized water) aqueous solution, deionized water (20.0 mg) and α -Al₂O₃ (20.0 mg) were put into a cylindrical fused silica cell (o.d. = 25 mm, i.d. = 23 mm, length = 250 mm) and stirred by a magnetic stirrer (1000 rpm) at 25 °C controlled by a heating jacket. Incident light from the UV-Vis spectrometer (Agilent Technologies Carry 5000) was focused on the cell and the reflected light was collected with concave mirrors and finally recorded by the detector in the spectrometer (Figures S2 and S3). α -Al₂O₃ was measured as a standard material for prior to the aimed measurement. Metal oxides with strong covalent bonds are insoluble in water. In addition, used α -Al₂O₃ possesses high crystallinity and purity as well as non-porous property (Fig. S4) with a band gap energy of 8.6 eV [2]. All these properties reflected no absorption in the studied range of 200-800 nm, and a very small capacity of adsorbing solutes thus, advantageous of using α -Al₂O₃ as the best candidate for a light-diffusing agent for our method. In contrast, other investigated metal oxides have narrower band gap energies and/or more impurities compared to α -Al₂O₃ yielding photo-absorption in the measured wavelength region (Fig. S5). It has to be mentioned that in the present study, generated gases of hydrogen and carbon dioxide from FADH reaction and water used as a solvent for FA and the catalyst have no photo-absorption in the region of measured wavelength.

The obtained diffuse reflectance spectra were transformed into absorption spectra through the Kubelka-Munk equation (Eq. 2), where R_∞ , K and S' represent diffuse reflectance, absorption coefficient of the specie and the scattering coefficient of particles (in the present case, reciprocal of average distance between the α -Al₂O₃ particles), respectively. The K/S value is directly proportional to the concentration of the species.

In the present study, concentrations of the focused solute molecules are discussed based on their absorption peak intensities instead of integrated absorption intensities, because the spectral widths and peak positions of the absorption bands from the common origin were insensitive to the concentrations. Prior to the analysis of the absorption spectra during FADH reaction, correlation function (calibration curve) between the concentration of FA aqueous solution and the peak intensity of the photo-absorption (215 nm) originating from FA using the new spectroscopic system was obtained. Using the correlation function, results in Figure 3 were obtained from Figure S11(b).

1.4 Formic Acid Dehydrogenation

To conduct the formic acid dehydrogenation, a solution consisted of 19.5 mL of H₂O, 8×10^{-4} mmol of [Cp*Ir(4DHBP)(OH₂)]SO₄ and 2.0 mmol of α -Al₂O₃, was added to the fused silica cell fitted with the heating jacket heated to the reaction temperature of 60 °C - 80 °C. The temperature of the sample was monitored by a temperature sensor (K type thermocouple) and it was recorded by a data logger (GL240, GRAPHTEC Co.). When the temperature reached the set value, 0.5 mL of FA was added to the test tube to start the reaction while UV-Vis-diffuse-reflectance spectra of the

sample were measured with the Cary 5000 spectrometer. The gas volume was measured with MilliGascounters (MGC-1, Ritter Engineering).

Figures

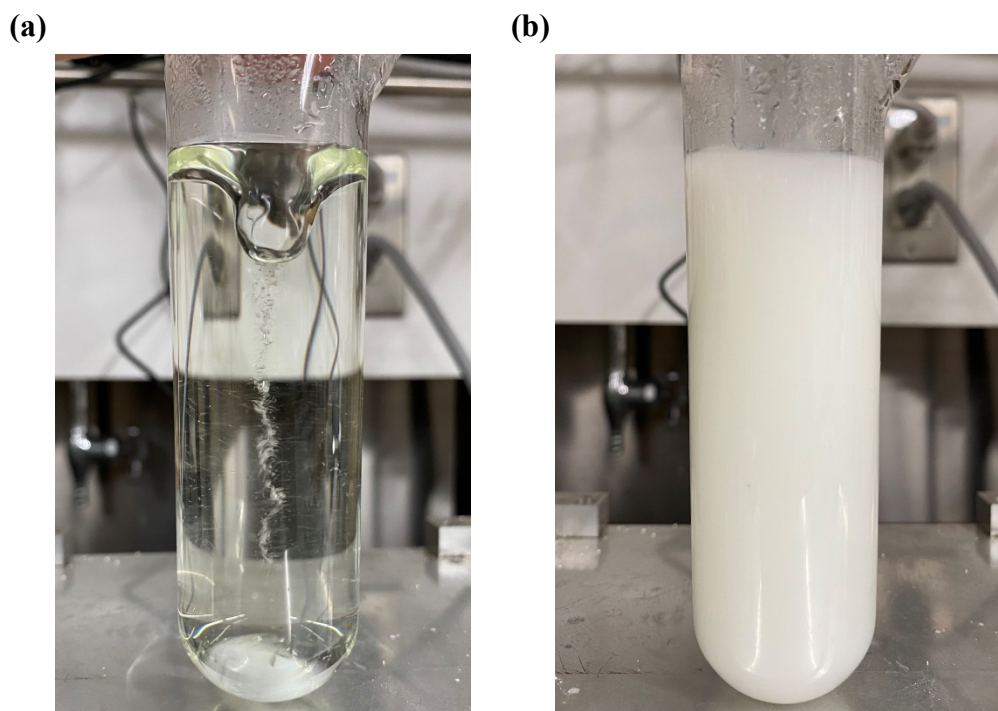


Fig. S1 Images of the cells (o.d. $\phi = 25$ mm, i.d. $\phi = 24$ mm) reactor containing aqueous solutions (0.5 mL of FA, 19.5 mL of H₂O) in during the FADH reaction in the presence of catalyst (8×10^{-4} mmol, 0.5 mg) at 80 °C (a) without α -Al₂O₃ particles; (b) with α -Al₂O₃ particles (200 mg) stirred by a magnetic stirrer (1000 rpm).

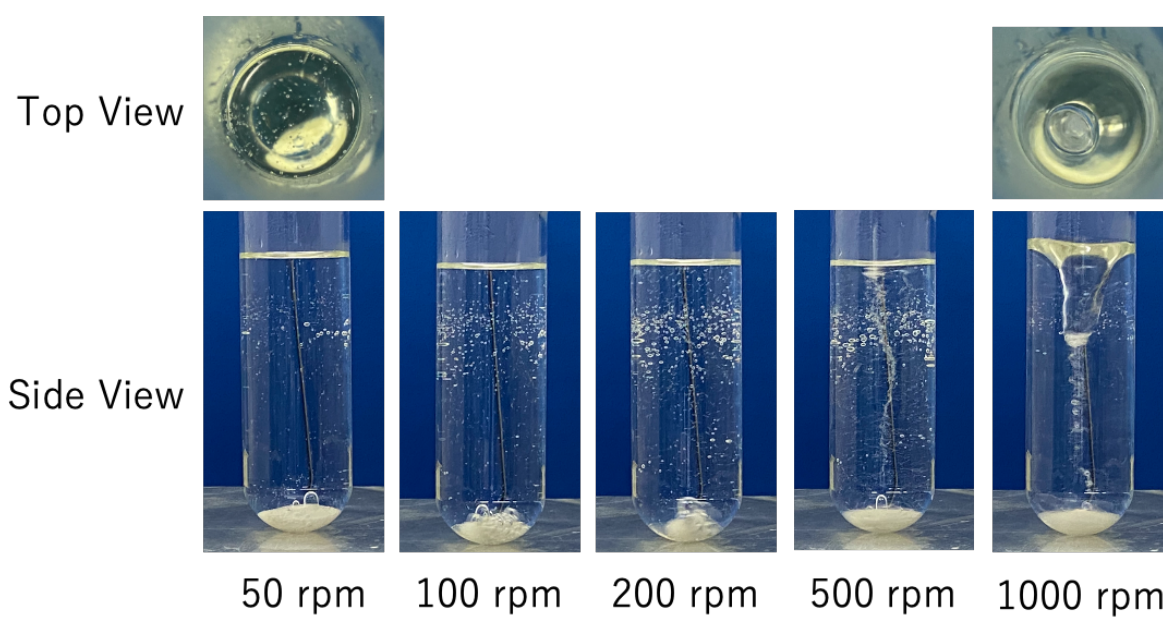


Fig. S2 The snapshots from top and side of the cell during the FADH at each stirring rate. Over 1000 rpm, most of the bubbles from FADH are concentrated to the center of the cell.

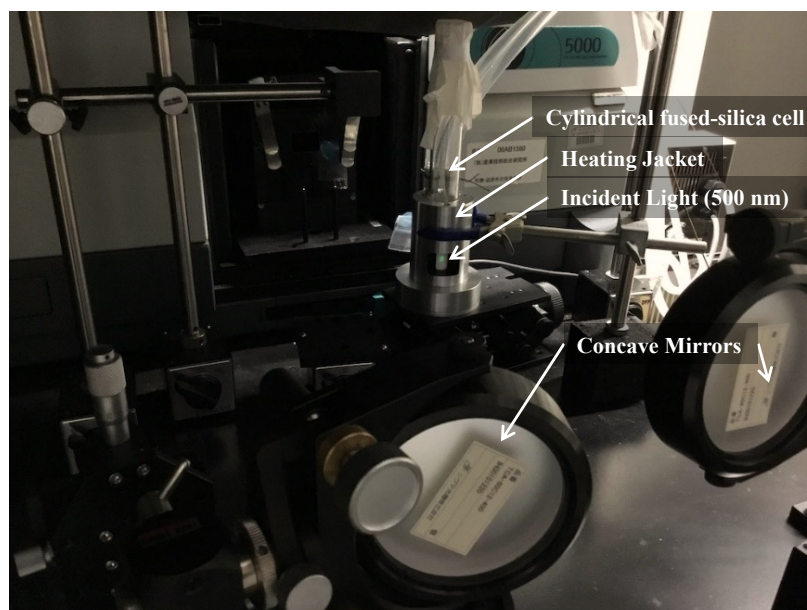


Fig. S3 The photo of the UV-Vis-diffuse-reflectance spectroscopy system which consists of Carry 5000 with concave mirrors and the cell with the heating jacket.

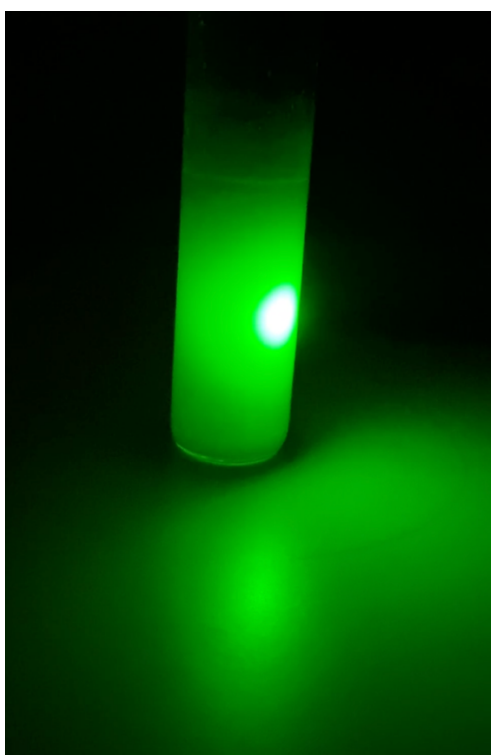


Fig. S4 The photo of the cylindrical cell with irradiated light (532 nm) from a laser pointer for demonstration.

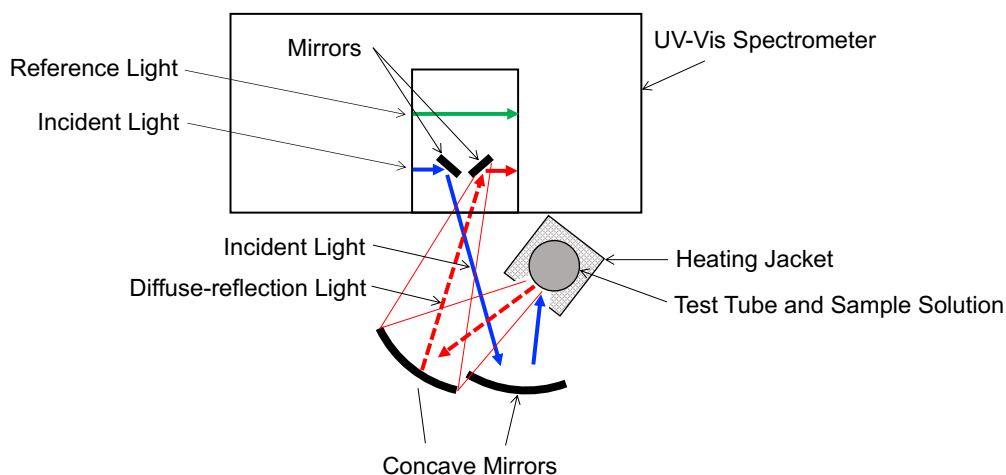


Fig. S5 The schematic top view of the UV-Vis-diffuse-reflectance spectroscopy system.

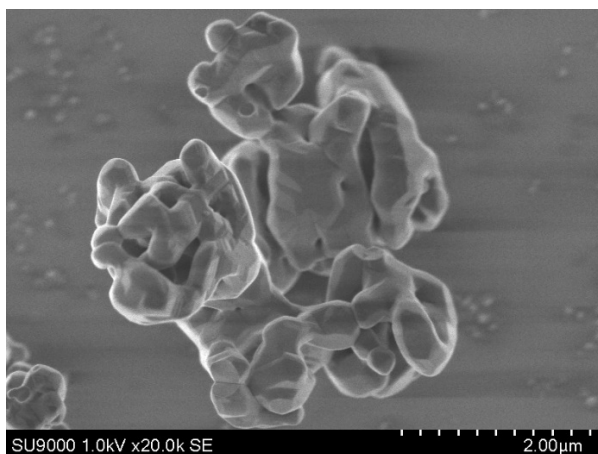


Fig. S6 The SEM image of α - Al_2O_3 used for the UV-Vis-diffuse-reflectance spectroscopy system.

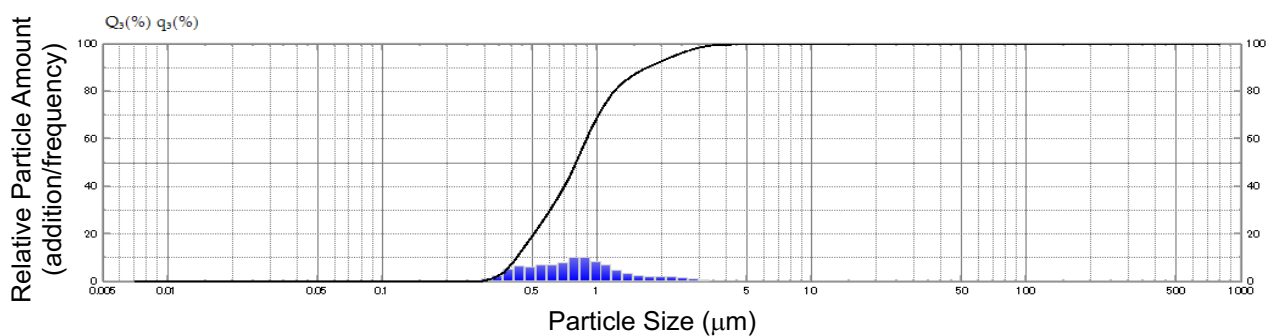


Fig. S7 The particle size distribution data from particle size analyzer (SALD-7500). The histogram and the solid line indicate particle size distribution and its integration on the particle number, respectively.

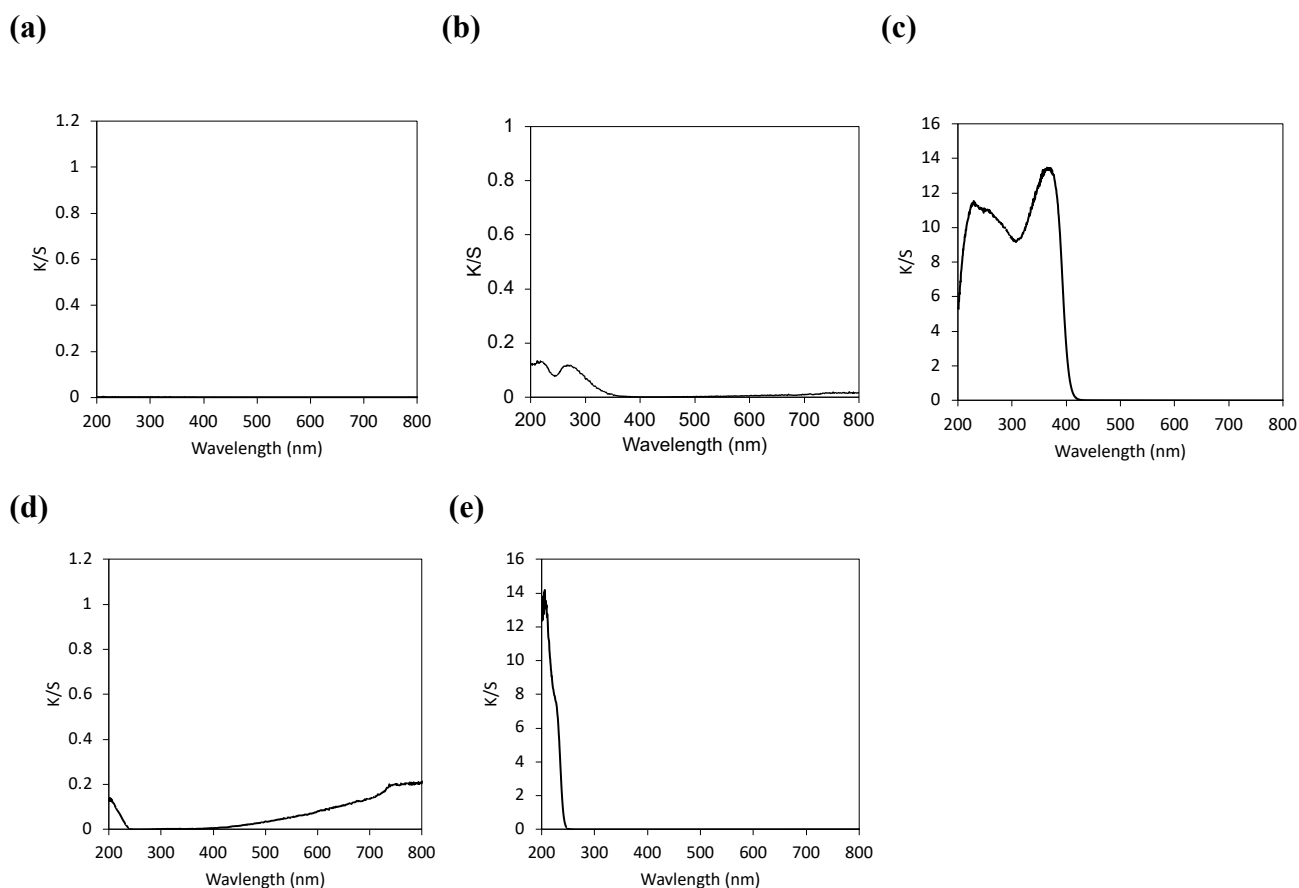


Fig. S8 The UV-Vis absorption spectra of (a) α - Al_2O_3 , (b) γ - Al_2O_3 , (c) SiO_2 (Si60), (d) TiO_2 (P25), (e) ZrO_2 (monoclinic) powders dispersed in water. α - Al_2O_3 was used as a standard.

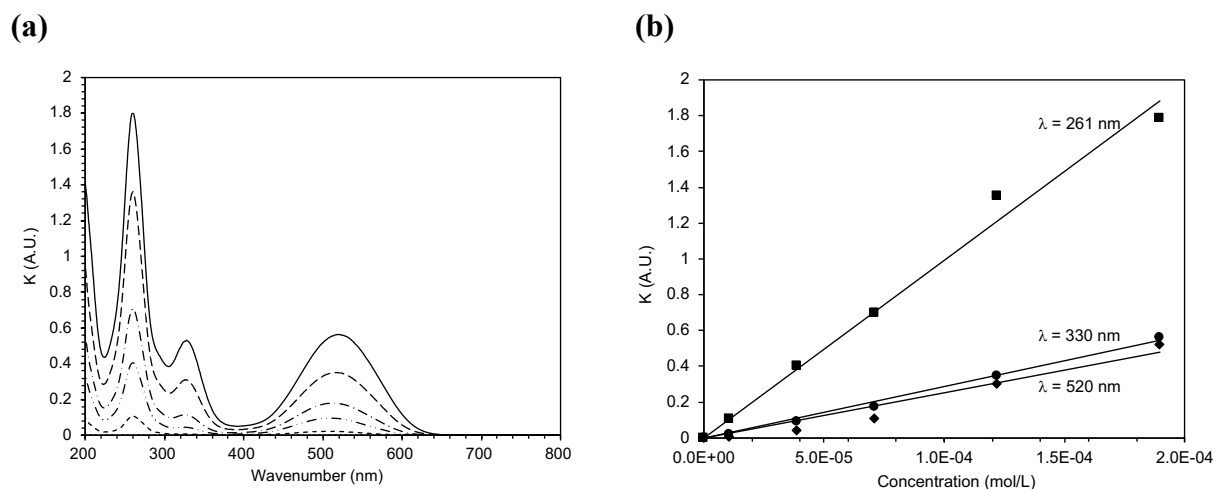


Fig. S9 (a) The UV-Vis diffuse-reflectance spectra of alizarin at 1.04×10^{-5} , 3.88×10^{-5} , 7.11×10^{-5} , 1.22×10^{-4} , and 1.90×10^{-4} mol/L, and (b) calibration lines between concentrations of alizarin and K values from the UV-Vis diffuse-reflectance spectra at each wavelength.

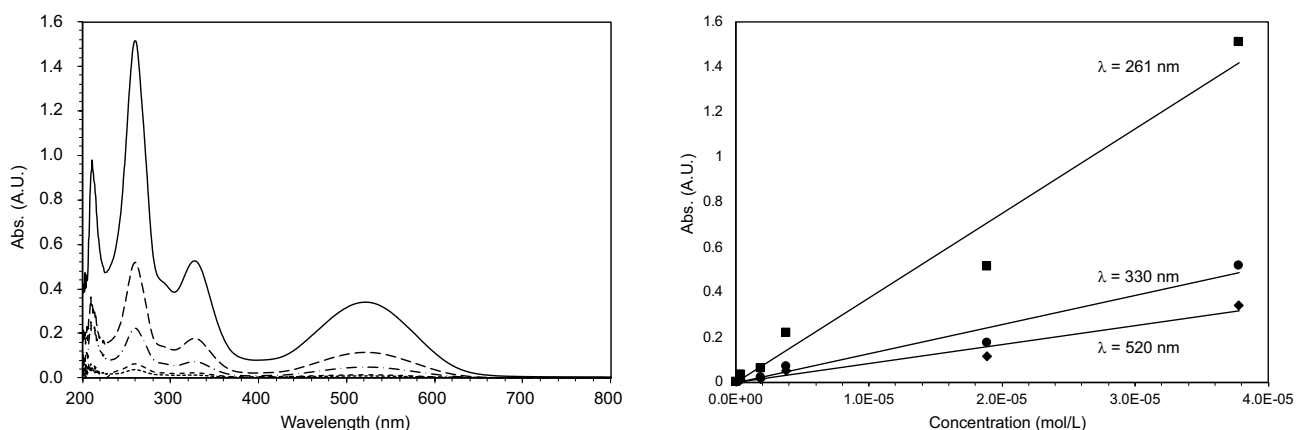


Fig. S10 (a) The UV-Vis transmittance absorption spectra of alizarin at concentrations of 3.78×10^{-7} , 1.89×10^{-6} , 3.78×10^{-6} , 3.78×10^{-5} , 1.89×10^{-5} mol/L, and (b) calibration lines between concentrations of alizarin and its absorption intensities at each wavelength.

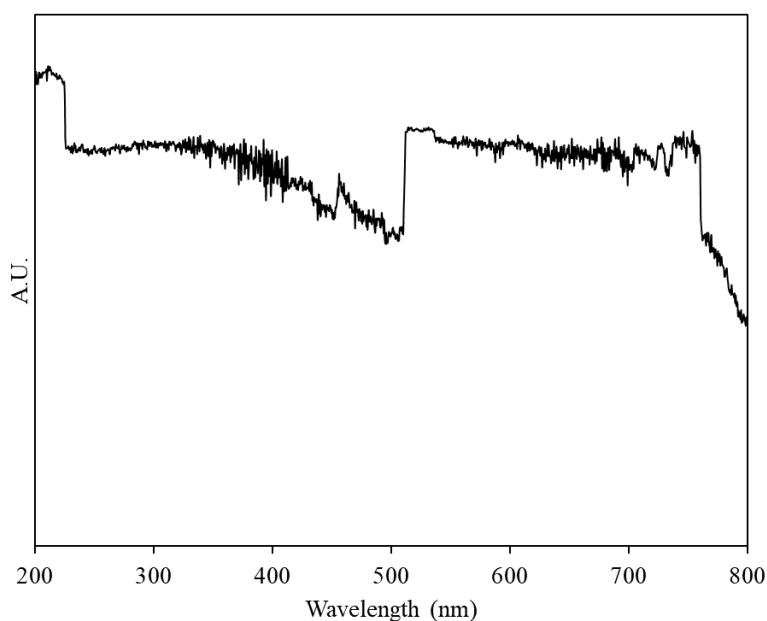


Fig. S11 The conventional transmission UV-Vis spectrum of the sample obtained during the FADH reaction. Hydrogen gas bubbles not only floating in the solution but those stuck to a sample glass cell and the fiber probe perturb the transmission of the incident light.

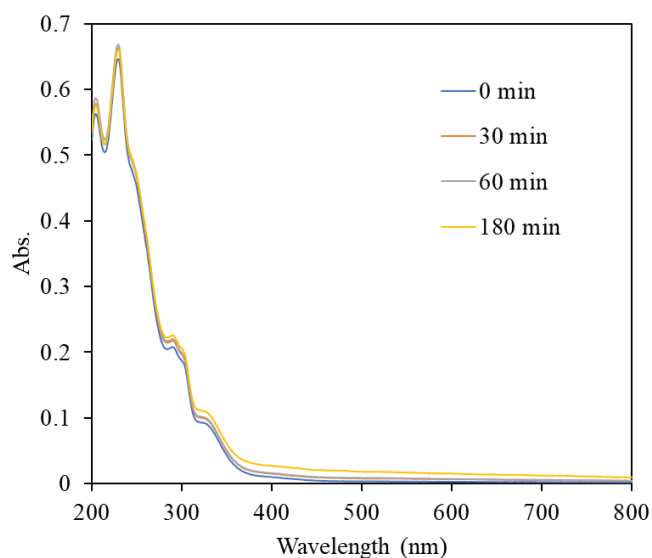


Fig. S12 The UV-Vis absorption spectra of the solutions after filtration. Experiment: We prepared four samples (20 mL) which consist of 0.01 M of H_2SO_4 , 40 μM of $[\text{Cp}^*\text{Ir}(\text{4DHBP})(\text{OH}_2)]\text{SO}_4$ and 0.1 M of $\alpha\text{-Al}_2\text{O}_3$. Then, the samples were stirred for 0 min, 30 mins, 60 mins and 180 mins, respectively. After the stirring, the samples were centrifuged for 20 mins (5000 rpm). Finally, their supernatants were measured by the conventional transmission UV-Vis spectroscopy.

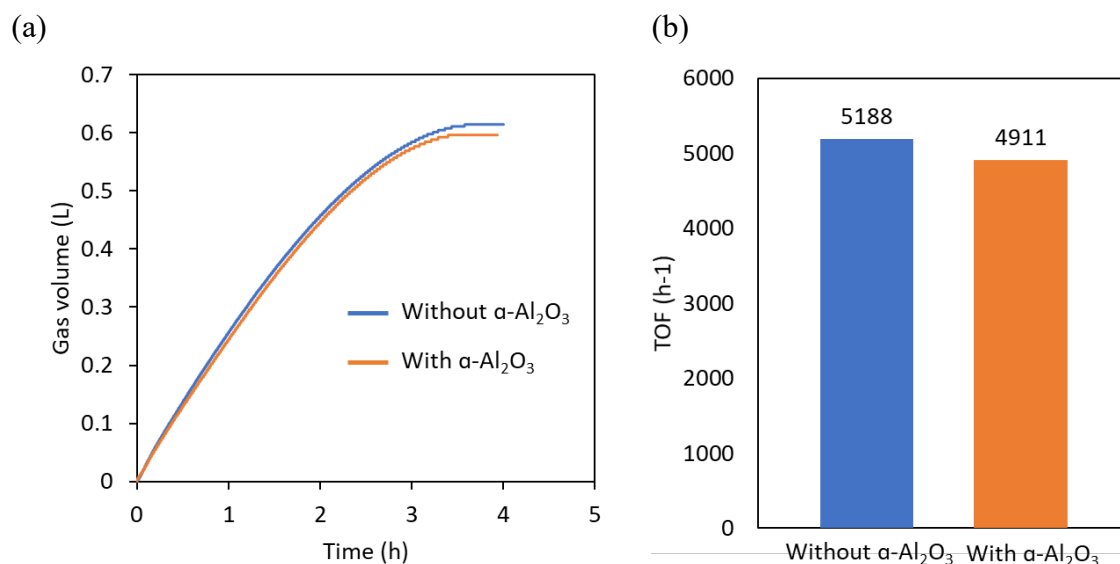


Fig. S13 (a) The time-course of total gas volume as a function of FADH reaction time without/with $\alpha\text{-Al}_2\text{O}_3$ measured by the gas meter; (b) The turnover frequency (TOF) of the sample without/with $\alpha\text{-Al}_2\text{O}_3$ calculated by using the data measured by the gas meter.

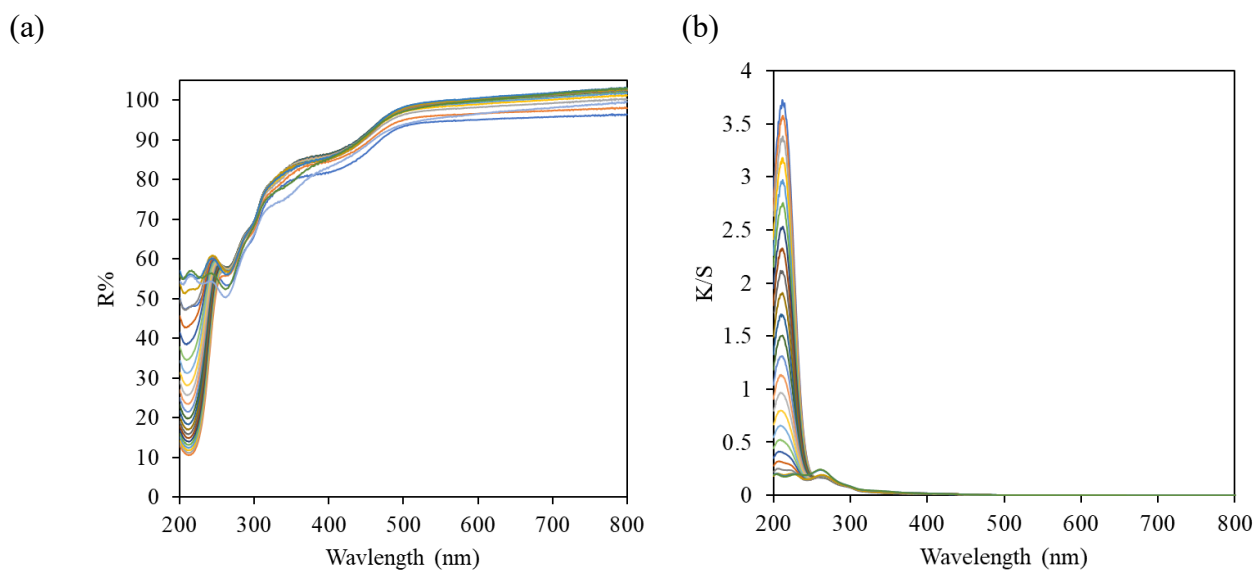


Fig.S14 (a) The diffuse reflectance spectra of the sample during the FADH reaction; (b) The absorption spectra of the sample during the FADH reaction. The sample (20 mL) consisted of 0.66 M of FA, 40 μ M of $[\text{Cp}^*\text{Ir}(\text{4DHBP})(\text{OH}_2)]\text{SO}_4$ and 0.1 M of $\alpha\text{-Al}_2\text{O}_3$.

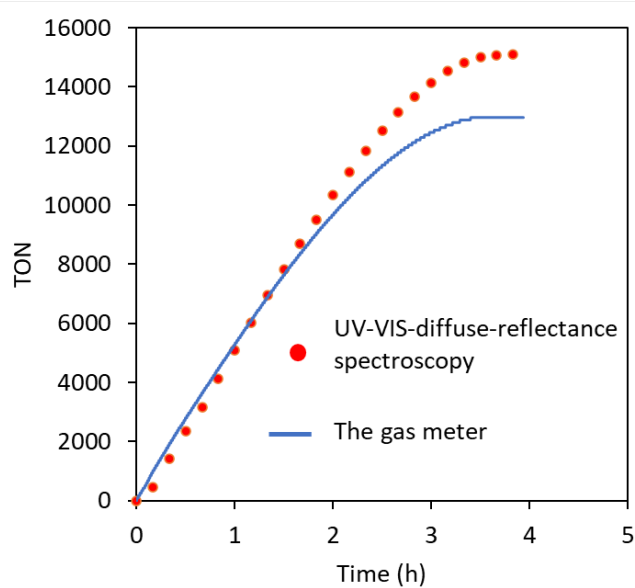


Fig. S15 The turnover number (TON) of the formic acid dehydrogenation reaction as a function of reaction time at 80 $^{\circ}\text{C}$ calculated by using the data of UV-Vis-diffuse-reflectance spectroscopy and that of the gas meter, respectively.

1. Huber, R., et al., *The Role of Surface States in the Ultrafast Photoinduced Electron Transfer from Sensitizing Dye Molecules to Semiconductor Colloids*. Journal of Physical Chemistry B, 2000. **104**: p. 8995-9003.
2. Wang, T., et al., *Band Gap and Band Offset of Ga_2O_3 and $(\text{Al}_x\text{Ga}_{1-x})_2\text{O}_3$ Alloys*. Physical Review Applied, 2018. **10**(1), 011003 1-7.